Chalcogenide Letters Vol. 12, No. 4, April 2015, p. 155 - 160

TEST OF MICROWAVE PLASMA SULFUR INCORPORATION AT CIGS SURFACE

T. CHEN*, Y. SUN

Institute of Photo-electronic Thin Film Devices and Technology ,Tianjin Key Laboratory of Thin Film Devices and Technology, Nankai University, Tianjin 300071, PR China

The test of microwave plasma sulfur incorporation at CIGS surface has been performed, the XRF results shows that this technique is efficient in incorporating sulfur at CIGS surface even at low substrate temperature (350 ℃) with a short processing time. GIXRD analysis of sulfurized samples confirms that CIGSSe phase is efficiently generated near the surface area, with the increase of substrate temperature, the content of CIGSSe phase could be increased and controlled. SEM cross-sectional images shows that microwave plasma sulfur incorporation can reduce the tiny grains remained at grain boundary and smooth the grain boundary surface. Microwave plasma sulfur incorporation shows its effectiveness in surface sulfurizing of CIGS.

(Received February 21, 2015; Accepted April 5, 2015)

Keywords: Microwave sulfur plasma, Effective sulfur incorporation, CIGSSe

1. Introduction

Incorporation of sulfur at the $Cu_2In_{(1-x)}Ga_xSe_2$ (CIGS) surface forms a thin layer of $Cu_2In_{(1-x)}Ga_xSe_{(2-y)}S_y$ (CIGSSe), which is proven to be effective in enhancing Voc and FF[1]. The sulfur surface incorporation expands surface band gap by lowering the valance band maximum without significantly affecting the conduction band minimum, carrier recombination in the space charge region can also be reduced by sulfur passivation of the interface donor defects[2, 3].

However, the incorporation of sulfur tends to be very difficult once the chalcopyrite grain is well grown after high temperature procesing. So to incorporate more sulfur into the CIGS, incomplete low temperature selenization followed by a high temperature sulfurization has been employed to incorporate sulfur into the CIGS, yet those possible secondary phases(mainly $Cu_{2-x}Se$) generated by low-temperature incomplete selenization could remain at the grain boundary if the sulfurization is not robust [4, 5].

Both elemental sulfur and H_2S has been employed as the sulfur source for incorporation, yet the high substrate temperature (above 500 ^oC) , long process time(typically over 30 min) and insufficient amount of incorporated sulfur shows the lack of incorporation effectiveness[6-9]. Simulation results have shown that, good performance of surface sulfurization requires effective sulfur incorporation within the space charge region without causing side effects[10, 11]. Based on our previous research on the microwave plasma sulfurization technique[12], we performed a test of microwave plasma sulfur incorporation at CIGS surface to see if this technique can incorporate sulfur effectively.

*Corresponding author: taichen_nku@sina.com

2. Experiment

In previously published work[12], we described the details of the microwave sulfur plasma reactor, which functions effectively for generating high reactivity S_2. To test the effectiveness of microwave plasma sulfur incorporation, we set up a contrast experiment between the microwave plasma sulfur incorporated sample C and non-plasma sulfur incorporated sample γ. The effect of the substrate temperature on the sulfur incorporation can be revealed by the analyzing samples(A,B,C). Detailed experiment parameters are listed in Table.1.

Table 1. Sulfur incorporation and samples processing parameters

Microwave plasma Incorporation (*)			Non-plasma Incorporation(#)
Microwave power		200W	0W
Sulfur heating		140℃	300℃
Ar Flow rate		5sccm	5sccm
Pressure		30Pa	40Pa
Sample ID	Incorporation Methods	Substrate Temperature	Processing Time
A	*	350℃	5 min.
B	*	450℃	5 min.
C	*	550℃	5 min.
γ	#	550℃	30 min.

The CIGS substrate is fabricated using the 3-step co-evaporation method. XRF test is utilized to analyze the composition of elements in all samples before and after the microwave plasma sulfur incorporation. Further GIXRD analysis is performed to confirm the effectiveness of microwave plasma sulfur incorporation. SEM cross-sectional image is taken to demonstrate the difference between sample γ and C.

3. Results and discussion

3.1 XRF analysis

In Table.2, XRF composition data of the samples(A,B,C, γ) before and after sulfur incorporation are listed. When the sulfurization parameter of sample A is 350 ^{o}C-5 min, the atomic composition of sulfur reaches 6.8%, it should be noted that, the S/(S+Se) ratio achieved by such a low substrate temperature(350 ^{o}C) and short processing time（5 min）reaches 0.13, while 2% H_2S mixed with Ar processing takes higher substrate heating temperature (525 ^{o}C) and longer processing time (120 minutes) to reach 0.14[7, 8], such difference should make a clear

demonstration of the effectiveness of plasma sulfur incorporation. When the substrate temperature is 450 ^{o}C， processing time remains 5 min, the S/(S+Se) increases to 0.235, a value only can be reached when CIGS is annealed in higher concentration H_2S ,higher substrate temperature or longer time[8, 9]. When the substrate temperature is 550 ^{o}C， processing time is 5min, the S/(S+Se) ratio of sample C reaches 0.38, while the S/(S+Se) ratio of sample γ is only 0.1 even with increased processing time (30 min) and sulfur evaporation temperature(300 ^{o}C). The contrast experiment of sample C and γ shows that microwave plasma sulfur incorporation is a feasible way to enhance the reactivity of elemental sulfur vapor, which makes microwave plasma cracked sulfur a more competitive sulfur source than toxic H_2S.

Table.2 XRF composition data of samples before and after sulfur incorporation

Sample ID	Chemical Composition (%) Before Sulfur Incorporation				Substrate Temp. (℃)	Chemical Composition (%) After Sulfur Incorporation				
	Cu	In	Ga	Se		Cu	In	Ga	Se	S
A	18.4	26.1	5.2	50.3	350*	17.7	24.4	4.8	46.3	6.8
B	24.1	16.2	8.8	50.9	450*	22.2	14.9	8.1	41.9	12.9
C	18.3	26.0	5.3	50.4	550*	15.2	20.4	4.2	37.5	22.7
γ	18.0	26.3	5.1	50.6	550$^{\#}$	17.8	25.1	4.8	46.9	5.4

3.2 GIXRD analysis

Fig.1 shows the GIXRD patterns of the CIGS sample without sulfur incorporation, the dominating phase is CIGS. As can be seen in Fig.1 the XRD pattern of 3-step co-evaporated CIGS is dominated mainly by the 3 diffraction peaks of CIGS, (112),(220) and (312). With the increase of incident angle, the X-ray penetration depth increases along with the intensity of diffraction peaks, the intensity of certain diffraction peak is proportional to the amount of certain phase exposed to incident X-ray. In our case, CIGS and CIGSSe are the two dominating compound, CIGS will be transformed into CIGSSe when Se atoms are replaced with S atoms, which means the increase of intensity of CIGSSe will lead to a decrease of the intensity of CIGS when the total amount of available CIGS is a constant. Such empirical rule only works with limited amount of phases (no more than 2), and the intensity change of certain diffraction peaks (CIGS or CIGSSe) should be able to provide some basic information of the amount change of these phases.

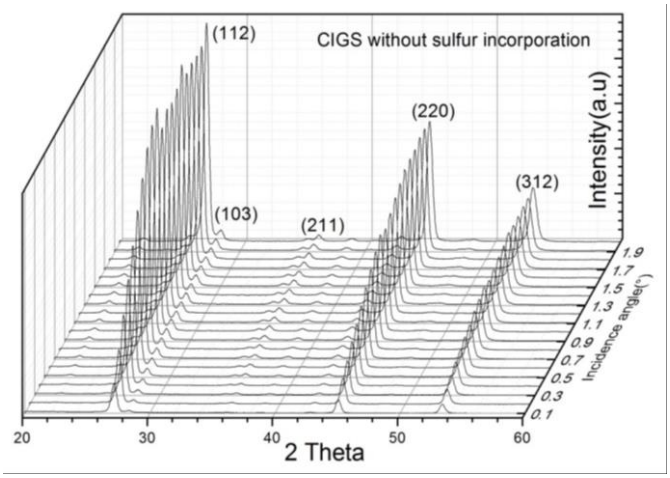

Fig.1. GIXRD patterns of CIGS without sulfur incorporation

In Fig.2 is the GIXRD pattern of sample A sulfurized with substrate temperature 350 °C, the (112),(220) and (312) diffraction peaks of CIGS are marked in black, the (112),(220) and (312) diffraction peaks of CIGSSe are marked in gray. As can be seen, the intensity ratio of CIGSSe (112) to CIGS (112) decreases gradually as the incident angle increases, which means the amount of CIGSSe decreases gradually from the surface of the film. This CIGSSe distribution pattern matches the one in report[8].

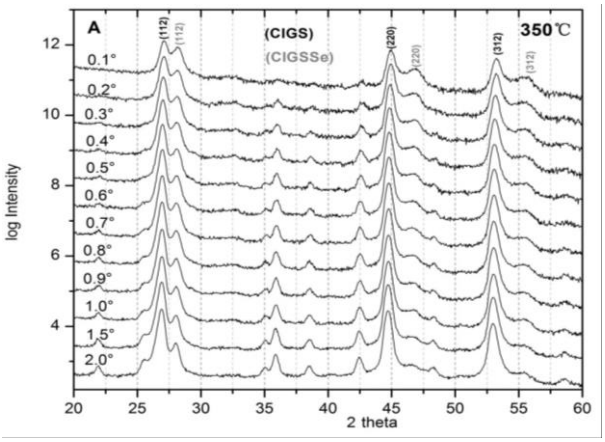

Fig.2 GIXRD patterns of sample A

Compare the GIXRD pattern of A and B, with the increase of substrate temperature from 350 °C to 450 °C, the intensity of CIGSSe diffraction peaks significantly increases, and become even stronger than the intensity of CIGS diffraction peaks at incident angles below 0.3°. This indicates that the amount of CIGSSe increases near the surface of the film. By comparing B and C, we could see that the intensity ratio of CIGSSe (112) to CIGS (112) remains above 1 until the incident angle increases over 1.0°. This indicates that more and deeper sulfur is incorporated into the CIGS when substrate temperature increases.

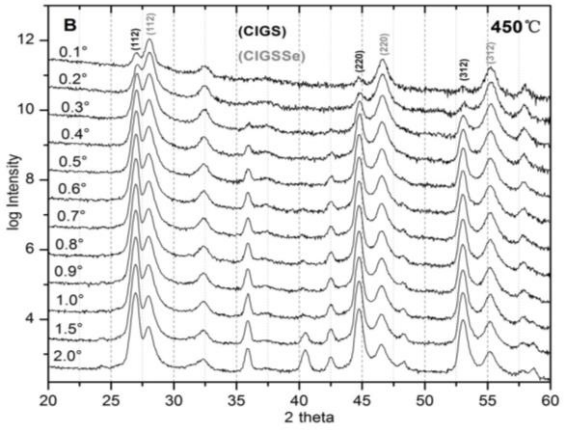

Fig.3. GIXRD patterns of sample B

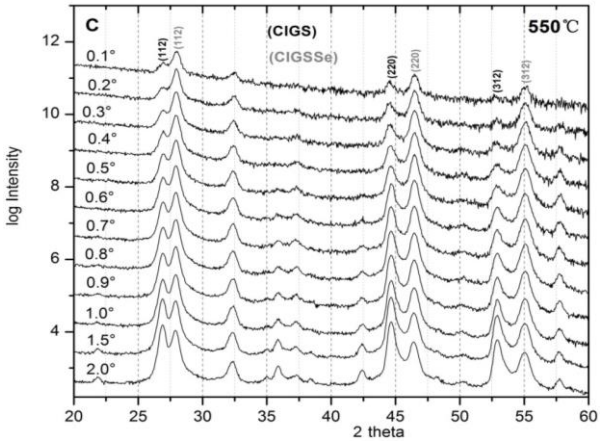

Fig.4. GIXRD patterns of sample C

From the GIXRD patterns of sample A, B and C, we could arrive at a conclusion that the CIGSSe phase is generated mostly near the surface of the film. Compare the sulfurized surface GIXRD with those in report at low incident angles (within 0.3°which penetrates the entire space charge region 250 nm), microwave plasma sulfur incorporation is efficient in incorporating sulfur even at relative low temperature(350 ^{o}C), and requires less processing time, such effectiveness should be attributed to the high reactivity of S_2 generated by microwave sulfur plasma .

3.3 SEM cross-sectional images

In Fig.5.shows the cross-sectional image of sample γ and sample C, the size of the grain in sample γ is not uniform, and tiny grains tend to accumulate at the grain boundary. In sample C, the grain is attaching the Mo without tiny grains at the grain boundary, and the surface of the grain boundary is smooth, this reduces the chances of carrier recombination. The reduced tiny grains at grain boundary and smoother surface may be attributed to incorporation of high reactivity sulfur which enhances the recrystallization.

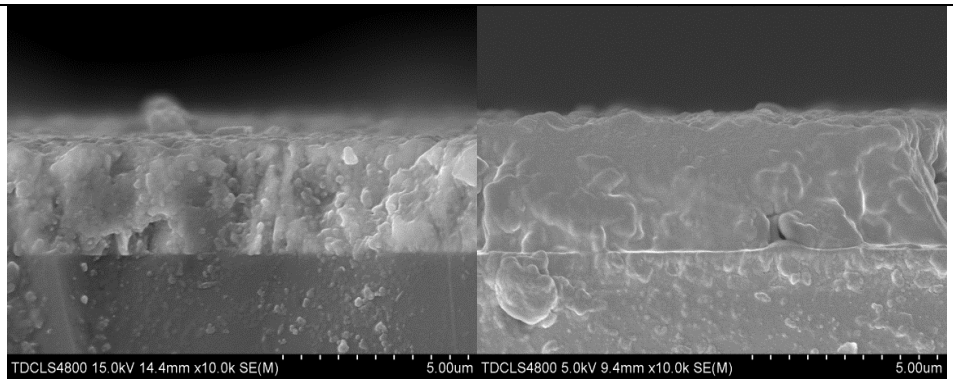

Fig.5. Cross-sectional images of sample γ (left) and C (right)

4. Conclusion

The XRF results shows that microwave plasma sulfur incorporation is efficient in incorporating sulfur at relatively low substrate temperature with short processing time. The GIXRD result further confirms that sulfur incorporation is efficient in transforming the CIGS into CIGSSe phase at surface area. With the increase of substrate temperature, more sulfur could be incorporated into CIGS. SEM cross-sectional images shows that microwave plasma sulfur incorporation is effective in reducing tiny grains at grain boundary.

References

[1] T. Kobayashi, H. Yamaguchi, Z. Jehl Li Kao, H. Sugimoto, T. Kato, H. Hakuma, T. Nakada, Progress in Photovoltaics: Research and Applications, pp. n/a-n/a, 2014.
[2] M. Turcu, I. M. Kötschau, U. Rau, Journal of Applied Physics, **91**, 1391 (2002).
[3] M. Turcu, U. Rau, Thin Solid Films, **431-432**, 158 (2003).
[4] B. Başol, A. Halani, C. Leidholm, G. Norsworthy, V. Kapur, A. Swartzlander, R. Matson, Progress in Photovoltaics: Research and Applications, **8**, 227 (2000).
[5] K. Kim, G. M. Hanket, T. Huynh, and W. N. Shafarman, Journal of Applied Physics, **111**, 083710 (2012).
[6] D. Ohashi, T. Nakada, and A. Kunioka, Solar Energy Materials and Solar Cells, **67**, 261 (2001).
[7] U. P. Singh, W. N. Shafarman, R. W. Birkmire, Solar Energy Materials and Solar Cells, **90**, 623 (2006).
[8] U. P. Singh, Vacuum, **83**, 1344 (2009).
[9] T. Nakada, H. Ohbo, T. Watanabe, H. Nakazawa, M. Matsui, A. Kunioka, Solar Energy Materials and Solar Cells, **49**, 285 (1997).
[10] C.-H. Huang, H.-L. Cheng, Numerical Simulation of Optoelectronic Devices (NUSOD), 2012 12th International Conference on, **27**, 117 (2012).
[11] Z. Jehl Li Kao, T. Kobayashi, T. Nakada, Solar Energy, **110**, 50 (2014).
[12] Y. S. T. Chen, Chalcogenide Letters **12**, 25 (2015).